

BNL-67631
 KEK Preprint 2000-68
 PRINCETON/HEP/2000-5
 TRI-PP-00-54

Search for the Decay $K^+ \rightarrow \pi^+ \pi^0 \nu \bar{\nu}$

S. Adler¹, M. Aoki^{5(a)}, M. Ardebili⁴, M.S. Atiya¹, P.C. Bergbusch^{5,7}, E.W. Blackmore⁵, D.A. Bryman^{5,7}, I-H. Chiang¹, M.R. Convery⁴, M.V. Diwan¹, J.S. Frank¹, J.S. Haggerty¹, T. Inagaki², M.M. Ito⁴, S. Kabe², S.H. Kettell¹, Y. Kishi³, P. Kitching⁶, M. Kobayashi², T.K. Komatsubara², A. Konaka⁵, Y. Kuno², M. Kuriki², T.F. Kycia^{1(b)}, K.K. Li¹, L.S. Littenberg¹, J.A. Macdonald⁵, R.A. McPherson⁴, P.D. Meyers⁴, J. Mildenberger⁵, N. Muramatsu², T. Nakano³, C. Ng^{1(c)}, T. Numa⁵, J.-M. Poutissou⁵, R. Poutissou⁵, G. Redlinger^{5(d)}, T. Sato², T. Shinkawa^{2(e)}, F.C. Shoemaker⁴, R. Soluk⁶, J.R. Stone⁴, R.C. Strand¹, S. Sugimoto², C. Witzig¹, and Y. Yoshimura²,
 (E787 Collaboration)

¹*Brookhaven National Laboratory, Upton, New York 11973*

²*High Energy Accelerator Research Organization (KEK), Oho, Tsukuba, Ibaraki 305-0801, Japan*

³*RCNP, Osaka University, 10-1 Mihogaoka, Ibaraki, Osaka 567-0047, Japan*

⁴*Joseph Henry Laboratories, Princeton University, Princeton, New Jersey 08544*

⁵*TRIUMF, 4004 Wesbrook Mall, Vancouver, British Columbia, Canada, V6T 2A3*

⁶*Centre for Subatomic Research, University of Alberta, Edmonton, Alberta, Canada, T6G 2N5*

⁷*Department of Physics and Astronomy, University of British Columbia, Vancouver, BC, Canada, V6T 1Z1*

Abstract

The first search for the decay $K^+ \rightarrow \pi^+ \pi^0 \nu \bar{\nu}$ has been performed with the E787 detector at BNL. Based on zero events observed in the kinematical search region defined by $90 \text{ MeV}/c < P_{\pi^+} < 188 \text{ MeV}/c$ and $135 \text{ MeV} < E_{\pi^0} < 180 \text{ MeV}$, an upper limit $B(K^+ \rightarrow \pi^+ \pi^0 \nu \bar{\nu}) < 4.3 \times 10^{-5}$ at 90% confidence level is established.

The flavor-changing neutral-current decay $K^+ \rightarrow \pi^+\pi^0\nu\bar{\nu}$ ($K_{\pi\pi\nu\bar{\nu}}$) is interesting because of its sensitivity to the combination of CKM mixing matrix elements $V_{ts}^*V_{td}$. Knowledge of the branching ratio, $B(K^+ \rightarrow \pi^+\pi^0\nu\bar{\nu})$, would provide additional constraints on quark mixing parameters, complementary to and independent of limits set by the related process $K^+ \rightarrow \pi^+\nu\bar{\nu}$. Within the framework of the Standard Model (SM), $K_{\pi\pi\nu\bar{\nu}}$ is dominated by short-distance contributions arising from one-loop penguin and box diagrams for $s \rightarrow d\nu\bar{\nu}$ mediated by charm and top quarks [1] [2]. Relating the hadronic matrix element of this decay to the measured isospin-rotated process $K^+ \rightarrow \pi^+\pi^-e^+\nu_e$ [3] minimizes hadronic uncertainties, making possible a theoretically clean prediction. However $K_{\pi\pi\nu\bar{\nu}}$ is highly suppressed by the GIM mechanism [4], as well as by phase space, so the SM prediction for the branching ratio is small, $B(K^+ \rightarrow \pi^+\pi^0\nu\bar{\nu}) = (1 - 2) \times 10^{-14}$ [5]. Because the present potential sensitivity for observing $K_{\pi\pi\nu\bar{\nu}}$ falls many orders of magnitude short of this predicted level, the primary motivation is the search for physics beyond the SM. Unlike $K^+ \rightarrow \pi^+\nu\bar{\nu}$, $K_{\pi\pi\nu\bar{\nu}}$ is sensitive to new physics mediated by axial-vector as well as by vector currents.

Because the ν and $\bar{\nu}$ are not directly observable, a full event reconstruction of $K_{\pi\pi\nu\bar{\nu}}$ is not possible. The signature is a single π^+ track, accompanied by two photons originating from the π^0 , with no other activity in the detector. A thorough accounting of all processes that can emulate the $K_{\pi\pi\nu\bar{\nu}}$ event topology and demonstration of the means to reject them allow sensitivity for observing $K_{\pi\pi\nu\bar{\nu}}$ decays.

E787 is a rare-kaon decay experiment at the Alternating Gradient Synchrotron (AGS) facility at Brookhaven National Laboratory (BNL). A prolific source of kaons is obtained by directing an intense beam of 24-GeV protons (typically 16×10^{12} per 1.6-second AGS spill) onto a 6-cm long platinum production target. A secondary beam containing 7×10^6 K^+ per spill is extracted at a momentum of 790 MeV/c [6]. Contaminants (i.e. π^+ and protons) are reduced by two stages of electrostatic separation to about 25% of the beam at the detector. Prior to entering the detector, beam particles are tracked and identified by a Čerenkov counter, two sets of multi-wire proportional chambers and a scintillation-counter hodoscope. They also pass through a BeO degrader that slows the kaons to 300 MeV/c. Approximately 20% of the incident kaons emerge from the degrader and enter the detector's stopping target.

The E787 spectrometer (see Figure 1) was designed to study the decay $K^+ \rightarrow \pi^+\nu\bar{\nu}$ [7]. This detector, however, is also well suited to look for other K^+ decay modes, including $K_{\pi\pi\nu\bar{\nu}}$. The cylindrically symmetric spectrometer is immersed in a 1-Tesla magnetic field provided by a solenoidal coil. The innermost radial section of the detector is a scintillating fiber target where incoming kaons come to rest. Segmentation of 5 mm \times 5 mm provides tracking of the K^+ and decay products in the target. Situated radially outward from the stopping target is a cylindrical drift chamber (UTC) [8], followed by a plastic-scintillator Range Stack (RS). The RS is segmented into 24 azimuthal sectors and 21 radial layers (a 6.35mm thick acceptance-defining layer followed by 20 19mm layers). Embedded within the RS are two layers of straw-tube chambers (RSSC) operated in limited-steamer mode. The RS photomultiplier tube (PMT) pulse shapes are recorded by 500-MHz flash-ADC transient digitizers (TDs) [9]. In addition to providing timing and energy information, the TDs provide pion identification by detecting the $\pi^+ \rightarrow \mu^+ \rightarrow e^+$ decay chain in the RS stopping counter.

The spectrometer is also equipped with an hermetic photon-detection system. The barrel

(BL) and endcap (EC) calorimeters, encompassing nearly 4π sr of solid angle, are used to detect γ pairs to reconstruct the π^0 .

Situated immediately outside the RS, which is one radiation length (X_0) thick, the BL is a $14.3\text{-}X_0$ thick cylindrical photon detector, segmented into 4 radial layers and 48 azimuthal sectors, which accounts for two thirds of the total photon coverage. Extending 1.9 m in length, each of the 192 BL counters is made up of alternating layers of 1-mm lead and 5-mm scintillator, read out by PMTs at both ends. Approximately 29% of the energy deposited in the BL is visible in its scintillator. Position measurements along z (*i.e.*, parallel to the beam) derive from both charge- and time-based information.

The two ECs on the upstream (US) and downstream (DS) ends of the detector account for the remaining third of the photon coverage [10]. Each EC consists of 4 concentric rings of undoped CsI crystals $13.5\text{-}X_0$ thick. Each EC module is viewed by a single PMT [11], whose pulse shape is recorded by 500-MHz CCD-based TDs [12]. Central holes (10.3-cm diameter US and 8.4-cm diameter DS) in the ECs accommodate the beam and target systems, respectively.

The photon veto encompasses a number of additional subsystems that fill minor openings along the beam direction, as well as any active parts of the detector not in the vicinity of the charged track. These are used in the data analysis to select γ showers that are confined to the BL and ECs and to reject background processes with additional photons.

The $K_{\pi\pi\nu\bar{\nu}}$ trigger [13] requires a kaon to enter the fiber target, and an online delayed coincidence (DC) of at least 1.5 ns is imposed to ensure that the kaon stops prior to its decay. The DC is also necessary to suppress background from scattered beam pions [14]. A single charged track is required to pass through the first two RS layers, penetrate to at least the sixth layer, and stop before the 19th layer. To differentiate pion from muon tracks online, the $\pi^+ \rightarrow \mu^+\nu_\mu$ decay signature is sought in the RS stopping counter by demanding that the TD pulse of the pion have a larger area, due to the decay muon, than a single pulse of the same height. Tracks reaching the outer three RS layers are also vetoed, which effectively suppresses $K^+ \rightarrow \mu^+\nu_\mu$ events. The only photon veto imposed in the trigger is the condition that rejects events with RS energy outside the region of the charged track that triggers the detector. The data set used for the signal search consists of 1.7×10^6 $K_{\pi\pi\nu\bar{\nu}}$ triggers from an exposure of about 1.3×10^8 stopped K^+ during 1995.

In the offline analysis, a delayed coincidence of 2 ns is imposed to remove residual events triggered by prompt beam pions. Events containing multiple beam particles are rejected via analysis of the beam counter and chamber systems. All events are required to pass the basic charged-track (CT) and π^0 reconstruction cuts. In the former, the CT is required to be well reconstructed in the target, UTC and RS. The total momentum of the CT (P_{π^+}) is determined by correcting the momentum measured in the UTC for the energy loss suffered by a π^+ with the observed track length in the target. The resulting resolution is 2.74 MeV/c for $K^+ \rightarrow \pi^+\pi^0$ (K_{π^2}) events. Detailed target tracking of the CT identifies events in which a decay π^+ scatters before reaching the UTC. To reject muons, a good TD double-pulse fit is required in the RS stopping counter, confirming the π^+ signature ($\pi^+ \rightarrow \mu^+\nu_\mu$). Additional muon rejection is obtained by demanding the independently measured CT kinematic quantities be consistent with those of a π^+ : (1) the UTC-measured momentum must match the RS range and energy and (2) the RS energy-deposition pattern must be consistent with that of a π^+ (this also suppresses events with a photon overlapping

the RS track).

Photon shower activity is identified in the various subsystems as hits in coincidence with the CT to within a few ns with energy above a low threshold (typically ~ 1 MeV). Photons are reconstructed by assembling BL and EC hits into clusters, according to the proximity of the struck modules. Reconstruction of the π^0 requires the number of photon clusters (N_γ) to be exactly two. Photon-veto (PV) cuts are imposed to improve the overall π^0 reconstruction by eliminating showers that originate in the RS, as well as to remove additional photons from radiative decays.

The copious decay $K_{\pi 2}$ is topologically identical to $K_{\pi\pi\nu\bar{\nu}}$. Thus the search for the latter must be confined to a region in which the two processes are kinematically distinct, *i.e.* where the π^+ and the π^0 are significantly softer than those from $K_{\pi 2}$. However $K_{\pi 2}$ still constitutes the dominant background, due to cases in which an inelastic scatter in the target down-shifts the π^+ energy and independently the observed π^0 energy fluctuates downward. For $K^+ \rightarrow \mu^+\pi^0\nu_\mu$ ($K_{\mu 3}$) and $K^+ \rightarrow \pi^+\pi^0\gamma$ ($K_{\pi 2\gamma}$), the π^0 and its charged partner are both naturally down-shifted by the presence of a third energetic particle (*i.e.* the neutrino in $K_{\mu 3}$ and the radiative photon in $K_{\pi 2\gamma}$). These backgrounds arise respectively by misidentifying the μ^+ as a π^+ in $K_{\mu 3}$, and missing the radiative photon in the $K_{\pi 2\gamma}$ decay. ‘‘Double-beam’’ events are associated with a second beam particle (K^+ or π^+) that interacts or decays such that only a soft π^+, π^0 pair is seen.

Signal extraction requires that the total background be suppressed to a small fraction of an event. Most backgrounds are directly determined from data; care is taken to avoid examination of potential signal events. For each background study, two independent high-rejection cuts (or sets of cuts) are employed. Each background type is separately enhanced by inverting one of these cuts. Thus the targeted background can be isolated and any *other* cuts can be safely tuned without fear of bias from exposure of signal events. The roles of the two cuts can then be reversed and the two rejections multiplied.

To improve the rejection of most backgrounds, a kinematic fit to a π^0 hypothesis is performed on events with two photons, using energies and directions from photon clustering. As a result, the resolution of the fitted π^0 energy (E_{π^0}) for $K_{\pi 2}$ events is $\sigma = 17.3$ MeV, compared with $\sigma = 27.8$ MeV for the raw measured E_{π^0} (see Figure 2). In addition, a cut on the χ^2 -converted probability, $Prob(\chi_{\pi^0}^2)$, from the kinematic fit discriminates against π^0 tail effects arising either from photons down-shifted in energy via shower leakage, or from accidental pairings in which a single π^0 photon combines with a random hit or a radiative photon from $K_{\pi 2\gamma}$. Such photon pathologies tend to have bad fits and can be removed with a $Prob(\chi_{\pi^0}^2)$ cut at 5%. The $Prob(\chi_{\pi^0}^2)$ distribution for $K_{\pi 2}$ events is shown in Figure 3.

Overlapping photon clusters responsible for certain ($N_\gamma > 2$) backgrounds (*e.g.*, $K_{\pi 2\gamma}$) typically have more hits than normal and can often be detected by a detailed examination of the hit pattern of each cluster. The γ -overlap cut set, OVLP, also exploits the fact that the presence of two (or more) photons in a single cluster is often indicated by a significant displacement between the two most energetic counters in that cluster. These cuts are effective in removing coalesced showers in the BL and EC.

In the case of $K_{\pi 2}$ (and double-beam¹) background, advantage is taken of the fact that

¹In general, the $K^+ \rightarrow \pi^+\pi^0$ background measurement technique is valid for all processes with a

the π^+ and the π^0 are measured by independent systems. Because $K_{\pi 2}$ yields mono-energetic decay products, to reach the signal region the π^+ must lose energy through hadronic scattering in the stopping target and at least one of the π^0 photons must suffer a downward fluctuation in observed energy². These phenomena can be partly suppressed by target and $Prob(\chi_{\pi^0}^2)$ cuts but these cuts alone provide only modest rejections on the π^+, π^0 kinematic tail events. Thus cuts on P_{π^+} and E_{π^0} are used in suppressing the $K_{\pi 2}$ background and estimating its residual. Figure 4 shows the acceptance “box” defined by these cuts. The expected $K_{\pi 2}$ background is found to be 0.044 ± 0.009 events in the $K_{\pi\pi\nu\bar{\nu}}$ search region for the present sample.

For $K_{\pi 2\gamma}$ background, both data and Monte Carlo were used to determine the number of $K_{\pi 2\gamma}$ events in the $K_{\pi\pi\nu\bar{\nu}}$ search region. In rejecting $K_{\pi 2\gamma}$, photon multiplicity, $Prob(\chi_{\pi^0}^2)$, PV, cluster-characteristics cuts (*e.g.*, on the number of hits in each cluster and OVLP), and cuts on photon overlap of the π^+ track are all useful. The dominant contribution is found to come from the inner bremsstrahlung (IB) component which yields < 0.01 events at 90% confidence level for the present data sample. The contribution from the direct emission (DE) component of $K_{\pi 2\gamma}$ is negligible. For $K_{\mu 3}$ background, one relies on muon rejection via the independent TD and π^+ kinematic-consistency cuts. The expected muon background is 0.024 ± 0.012 events.

The total expected background from all sources is 0.068 ± 0.021 events. Validation checks for the $K_{\pi 2}$ and $K_{\mu 3}$ background estimates were carried out by examining events outside but near the P_{π^+} vs E_{π^0} box. This requires relaxing cuts and comparing the estimated number of residual events with the results of actual examination of the exterior neighborhood of the $K_{\pi\pi\nu\bar{\nu}}$ box. Good agreement is obtained between the background predictions and the number of events observed for several larger boxes. The $K_{\pi 2}$ outside-the-box background study results are shown in Table I as an example.

After imposing the complete set of cuts, no events are observed in the search region defined by $90 \text{ MeV}/c < P_{\pi^+} < 188 \text{ MeV}/c$ and $135 \text{ MeV} < E_{\pi^0} < 180 \text{ MeV}$, as shown in Figure 4.

The total acceptance for the $K_{\pi\pi\nu\bar{\nu}}$ analysis is determined to be 0.0021 ± 0.0001 . Losses due to delayed coincidence, π^+ and π^0 reconstruction, timing (beam and photon vetoes), TD and π^+ kinematic consistency cuts, and $Prob(\chi_{\pi^0}^2)$ and γ -cluster pattern-related cuts are all determined from data. The Monte Carlo is used only to determine acceptances associated with the trigger, π^+ nuclear-interaction and decay-in-flight losses, and the kinematic box cut. These factors are listed in Table II. A more detailed description of the analysis can be found in Reference [15].

Finally, the signal sensitivity is ascertained through the ratio of the numbers of acceptance corrected $K^+ \rightarrow \pi^+\pi^0\nu\bar{\nu}$ and $K^+ \rightarrow \pi^+\pi^0$ events, both measured from the same $K_{\pi\pi\nu\bar{\nu}}$ data set. The majority of the cuts used for the $K_{\pi 2}$ event selection are similar to those employed in the $K_{\pi\pi\nu\bar{\nu}}$ analysis so that systematic errors incurred in the acceptance measurements tend to cancel. The major differences are in the kinematic box cut which

π^+, π^0 pair, which includes double beam background.

²The $\gamma\gamma$ opening angle must have a compensating error to keep $m_{\gamma\gamma} \approx m_{\pi^0}$.

in this case is tuned for a π^+ that is monoenergetic, an additional fiducial cut on the π^+ angle with respect to the beam direction, and kinematic cuts exploiting the monoenergetic nature of the π^0 . The number of surviving K_{π^2} events is 101775, corresponding to a total acceptance of 0.019 ± 0.001 . Based on zero events found in the $K_{\pi\pi\nu\bar{\nu}}$ signal region and the K_{π^2} branching ratio, 0.2116 ± 0.0014 [16], we set a 90% confidence level (c.l.) upper limit $B(K^+ \rightarrow \pi^+\pi^0\nu\bar{\nu}) < 4.3 \times 10^{-5}$.

The present data can also be used to limit the branching ratio for the process $K^+ \rightarrow \pi^+\pi^0 X^0$ where X^0 is a single non-interacting particle. Since this is a three-body decay, the extraction of such limits depends on the assumed matrix element. Figure 5 shows the 90% c.l. upper limit as a function of X^0 mass under the assumption of phase space³.

There are good prospects to improve these limits further. First, the total E787 data set obtained in 1995-8 has approximately five times the sensitivity of the search reported here. Second, a new experiment, E949 [17], now in preparation at BNL could yield further gains by virtue of its much larger exposure of K^+ and from trigger optimization.

We gratefully acknowledge the dedicated effort of the technical staff supporting this experiment and of the Brookhaven AGS Department. This research was supported in part by the U.S. Department of Energy under Contracts No. DE-AC02-98CH10886, W-7405-ENG-36, and grant DE-FG02-91ER40671, by the Ministry of Education, Science, Sports and Culture of Japan through the Japan-U.S. Cooperative Research Program in High Energy Physics and under the Grant-in-Aids for Scientific Research, for Encouragement of Young Scientists and for JSPS Fellows, and by the Natural Sciences and Engineering Research Council and the National Research Council of Canada.

³Testing a few plausible matrix elements resulted in upper limits that were comparable or lower.

REFERENCES

- (a) Now at KEK.
 - (b) Deceased.
 - (c) Also at Department of Physics and Astronomy, State University of New York at Stony Brook, Stony Brook, NY 11794-3800.
 - (d) Now at BNL.
 - (e) Now at the National Defense Academy of Japan, 1-10-20 Hashirimizu, Yokosuka, Kanagawa 239-8686, Japan.
- [1] T. Inami and C.S. Lim, Prog. Theo. Phys. **65**, 297 (1981); G. Buchalla, A. Buras and M. Harlander, Nucl. Phys. B **349**, 1 (1991); G. Buchalla and A. Buras, Nucl. Phys. B **412**, 106 (1994).
 - [2] C. Q. Geng, I. J. Hsu and Y. C. Lin, Phys. Rev. **D54**, 877 (1996).
 - [3] L. Rosselet *et al.*, Phys. Rev. D **15**, 575 (1977).
 - [4] S.L. Glashow, J. Iliopoulos and L. Maiani, Phys. Rev. D **2**, 1285 (1970).
 - [5] L.S. Littenberg and G. Valencia, Phys. Lett. B **385**, 379 (1996); see also C. Q. Geng, I. J. Hsu and Y. C. Lin, Phys. Rev. **D50**, 5744 (1994) and C. Chiang and F. J. Gilman, hep-ph/0007063 for work on closely related processes.
 - [6] J. Doornbos *et al.*, Nucl. Instrum. Methods Phys. Res. A **444**, 546 (2000).
 - [7] M.S. Atiya *et al.*, Nucl. Instrum. Methods Phys. Res. A **321**, 129 (1992); S. Adler *et al.*, Phys. Rev. Lett. **79**, 2204 (1997); S. Adler *et al.*, Phys. Rev. Lett. **84**, 3768 (2000).
 - [8] E.W. Blackmore *et al.*, Nucl. Instrum. Methods Phys. Res. A **404**, 295 (1998).
 - [9] M.S. Atiya *et al.*, Nucl. Instrum. Methods Phys. Res. A **279**, 180 (1989).
 - [10] I-H. Chiang *et al.*, IEEE Trans. Nucl. Sci. **NS-42**, 394 (1995).
 - [11] T.K. Komatsubara *et al.*, NIM **A404**, 315 (1998).
 - [12] D.A. Bryman *et al.*, Nucl. Instrum. Meth. A **396** 394 (1997).
 - [13] The trigger used for $K^+ \rightarrow \pi^+\pi^0\nu\bar{\nu}$ was primarily devised to accumulate data for calibrations and acceptance measurements and was prescaled by a factor 8656. It was not optimized for $K_{\pi\pi\nu\bar{\nu}}$ decay. A requirement that the π^+ reach the sixth layer of the RS is particularly restrictive for this four-body decay.
 - [14] In the absence of such a cut, beam pions which undergo hadronic scattering in the fiber target and are redirected toward the RS can trigger the system.
 - [15] C.F. Ng, *The Search for the Rare Decay $K^+ \rightarrow \pi^+\pi^0\nu\bar{\nu}$* , State University of New York at Stony Brook Ph.D. thesis, 2000.
 - [16] Review of Particle Physics, Particle Data Group, D.E. Groom *et al.*, The European Physical Journal **C15**, 1 (2000).
 - [17] B. Bassalleck *et al.*, E949 Proposal, BNL-67247, TRI-PP-00-06, August 1999.

TABLES

Outside-the-Box $K^+ \rightarrow \pi^+\pi^0$ Background Study		
OUTBOX Definition	Background Expectation	# Events Observed
$188 < P_{\pi^+} < 194$ $180 < E_{\pi^0} < 190$	0.127	0
$188 < P_{\pi^+} < 200$ $180 < E_{\pi^0} < 210$	14.6	16
$188 < P_{\pi^+} < 203$ $180 < E_{\pi^0} < 225$	423	433

TABLE I. Outside-the-box $K^+ \rightarrow \pi^+\pi^0$ background results (see text).

Acceptance Factors	$K_{\pi\pi\nu\bar{\nu}}$	$K_{\pi 2}$
$K^+ \rightarrow \pi^+\pi^0\nu\bar{\nu}$ trigger acceptance	0.060	0.446
Kinematic box acceptance	0.644	0.966
π^+ fiducial cut	na	0.967
π^0 kinematic cuts	na	0.925
π^+ nuclear interaction and decay-in-flight *	0.778	0.681
π^+ reconstruction efficiency*	0.944	0.944
Delayed coincidence cut*	0.803	0.803
π^+ target tracking, dE/dx, and timing cuts*	0.357	0.359
π^+ kinematic consistency cuts*	0.943	0.970
Transient digitizer ($\pi \rightarrow \mu$) cuts*	0.402	0.401
Photon cluster pattern cuts*	0.946	0.945
Requirement of two good photon clusters*	0.851	0.850
$Prob(\chi_{\pi^0}^2)$ cut*	0.852	0.852
Total acceptance	0.0021	0.019

TABLE II. Acceptance factors for $K^+ \rightarrow \pi^+\pi^0\nu\bar{\nu}$ ($K^+ \rightarrow \pi^+\pi^0$). Starred entries (*) indicate factors that are the same or closely related in $K_{\pi\pi\nu\bar{\nu}}$ and $K_{\pi 2}$ so that errors in their determination tend to cancel in the ratio. ‘na’ means not applicable

FIGURES

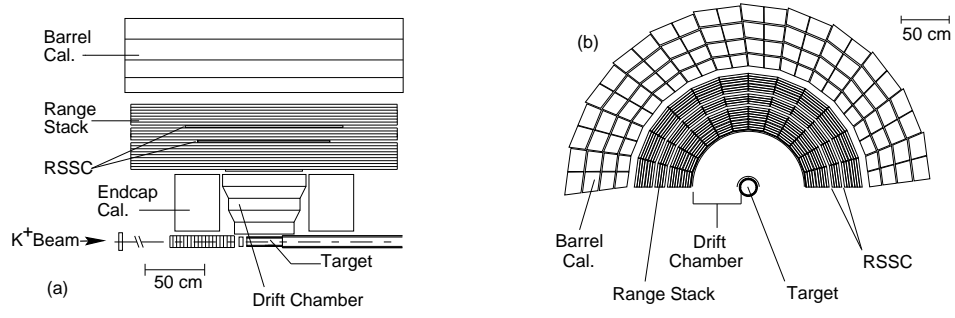


FIG. 1. Side-view (a) and end-view (b) of the upper half of the E787 detector.

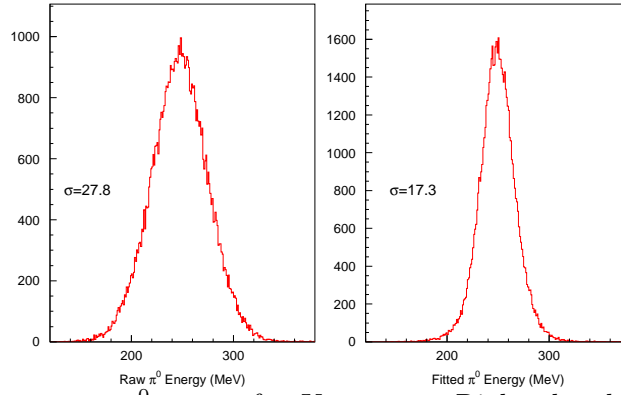


FIG. 2. Left plot shows raw π^0 energy for $K_{\pi 2}$ events. Right plot shows the π^0 energy for the same sample after the kinematic fit.

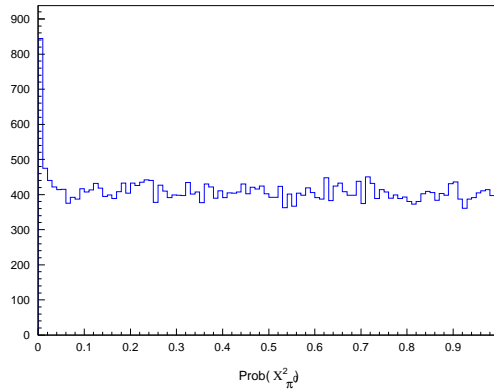


FIG. 3. Confidence level, $Prob(\chi^2_{\pi^0})$, for $K_{\pi 2}$ events.

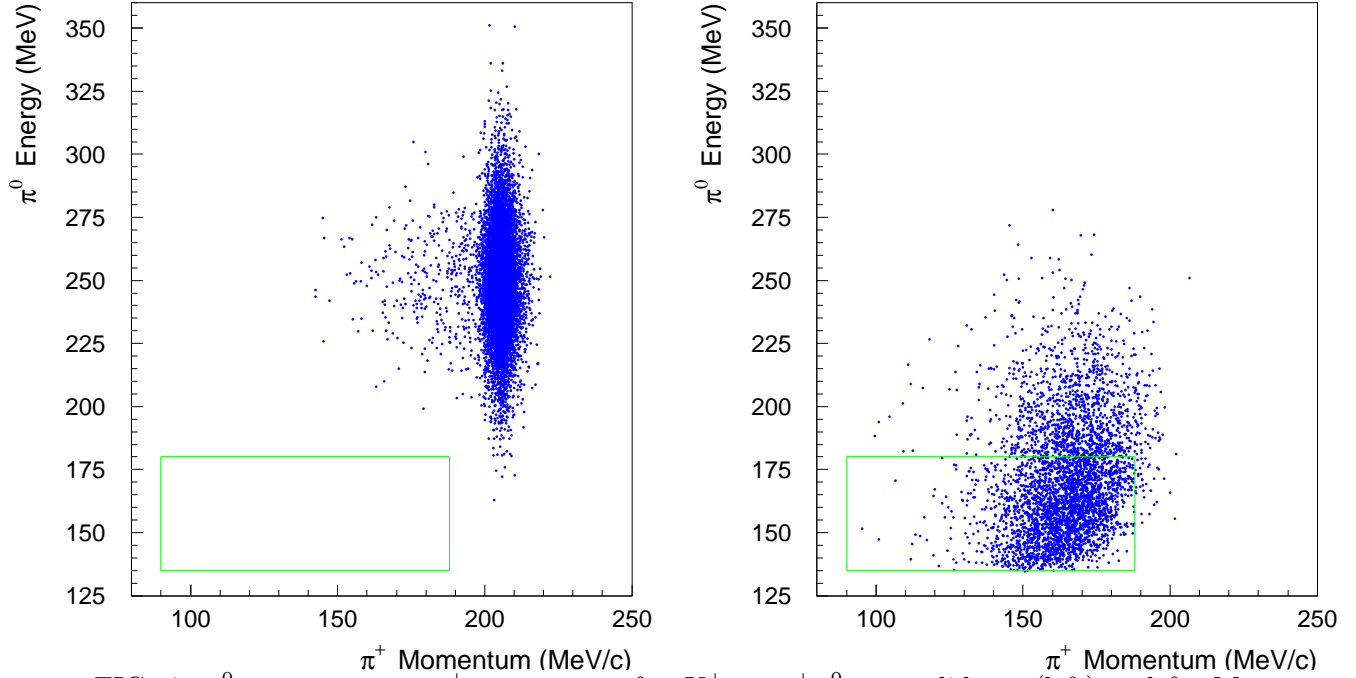


FIG. 4. π^0 energy versus π^+ momentum for $K^+ \rightarrow \pi^+\pi^0\nu\bar{\nu}$ candidates (left) and for Monte Carlo signal events (right). Box indicates the signal acceptance region. $K_{\pi 2}$ events cluster at the upper right in the top plot.

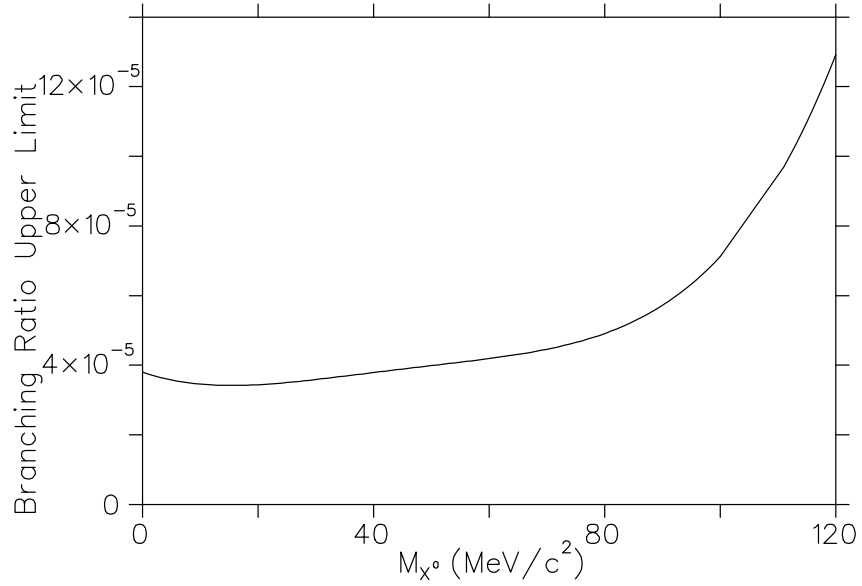


FIG. 5. The 90% c.l. upper limit for $B(K^+ \rightarrow \pi^+\pi^0 X^0)$ for a three-body phase-space decay model.